

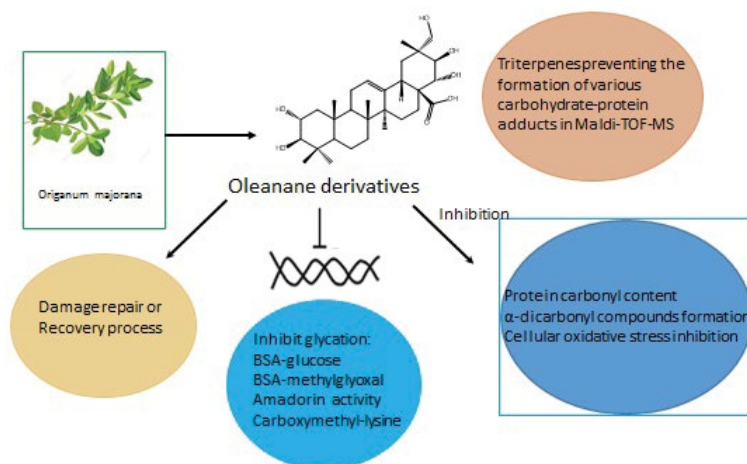
Protective Effects of Oleanane and Ursane Type Triterpenoids from *Origanum majorana* Against the Formation of Advanced Glycation Endproducts

Rosa Martha Pérez Gutiérrez*, Jahel Valdes Saucedo, Jose Maria Mota Flores and Blanca Elizabeth Lopez Silva

Research Laboratory of Natural Products, School of Chemical Engineering and Extractive Industries-IPN, Unidad Profesional Adolfo Lopez Mateos, Zacatenco, D.F. CP 07758, Mexico

Abstract

Bioassay guided fractionation of a crude methanol extract of leaves of *Origanum majorana* led the isolation of six new triterpenes (1-6). The structures of the isolates were established on the basis of extensive 1D and 2D NMR spectroscopic data interpretation and by comparison with those previously reported in the literature as 3 β ,11 α ,16 β ,21 β -tetrahydroxy-olean-12-en-28-oic acid (1), 2 α ,3 β ,21 β ,22 α ,29 α -pentahydroxy-olean-12-en-28-oic acid (2), 3 β ,15 α ,21 α -trihydroxyolean-olean-12-en-28-oic acid (3), 2 α ,29 α -diacetoxyl-3 β ,23 α -dihydroxy-olean-5,12-dien-28-oic acid (4), 3 β ,15 α ,23 α ,19 α -tetrahydroxyursan-12-ene-28-oic acid (5) and 2 α ,3 β -diacetoxyl-ursan-12,19-diene (6). Six other known triterpenes were isolated including oleanolic acid (7), 28-norlup-20(29)-ene-3 β ,17 β -diol (8), 3 β ,6 β ,7 β -trihydroxy-20(29)lupine-ene (9), ursolic acid (10), 3 β ,15 α ,dihydroxy-30-norurs-12-ene (11), and lupeol (12). All of the isolates were subjected *in vitro* bioassays to evaluate their inhibitory activity on the formation of advanced glycation end products (AGEs) including AGEs-BSA, methylglyoxal, Amadorin activity, carboxymethyl-lysine, protein carbonyl content, α -dicarbonyl compounds formation, cellular oxidative stress inhibition and protein structural changes were evaluated by Maldi-TOF-MS. Triterpenes 1-5 displayed inhibitory effects on these specific AGEs, more effectively than the positive control, aminoguanidine. Among these, compounds 2, and 1 exhibited the most potential inhibitory activity against AGEs formation. This activity is attributed in part to carbonyl scavenging capacities. This edible plant may be used for controlling oxidative stress and inhibiting the AGE formation, which are implicated in the pathogenesis of diabetic complications (Image 1).



Keywords: *Origanum majorana*; Protein glycation; Triterpenes; Ursane; Oleanane

Introduction

Glycation, a nonenzymatic reaction between reducing sugars and lysine residues is an important source of reactive carbonyl species (RCS) that leads to the formation of protein advanced glycation end products (AGEs) such as N ϵ -carboxymethyllysine (CML), methylglyoxal lysine dimers and glyoxal lysine dimers [1]. These adducts are formed in all stages of the glycation process, by Schiff's bases in early glycation, or degradation of glucose or Amadori products (fructosamine) in the intermediate stages of glycation. Thus, α -dicarbonyl could be considered very important to understand how glucose can form AGEs by the Maillard reaction [2]. Methylglyoxal and glyoxal are reactive dicarbonyl species (RCS) common intermediates in protein damage. In the presence of protein dicarbonyl compounds, reducing sugars and transition metal ions, can auto-oxidize to form superoxide radical that

can subsequently be converted to hydroxyl radical which is highly toxic. Lipoxidation, AGEs, reactive oxygen species (ROS) generation can provoke tissue damage and activate inflammation [3]. The hyperglycaemia

***Corresponding author:** Rosa Martha Pérez Gutiérrez, Research Laboratory of Natural Products, School of Chemical Engineering and Extractive Industries-IPN, Unidad Profesional Adolfo Lopez Mateos, Zacatenco, D.F. CP 07758, Mexico, Tel: +5296000 ext 55142; E-mail: rmpg@prodigy.net.mx

Received January 22, 2016; **Accepted** February 15, 2016; **Published** February 19, 2016

Citation: Pérez Gutiérrez RM, Saucedo JV, Mota Flores JM, Lopez Silva BE (2016) Protective Effects of Oleanane and Ursane Type Triterpenoids from *Origanum majorana* Against the Formation of Advanced Glycation Endproducts. Med chem (Los Angeles) 6: 095-114. doi:10.4172/2161-0444.1000333

Copyright: © 2016 Pérez Gutiérrez RM, et al. This is an open-access article distributed under the terms of the Creative Commons Attribution License, which permits unrestricted use, distribution, and reproduction in any medium, provided the original author and source are credited.

en diabetic can increase the production of free radicals and reactive oxygen species [4]. Glycation, is increased in hyperglycemic leading to an acceleration of AGEs [5]. Increased oxidative stress and accumulation of AGEs can induce cellular changes producing diseases, such as diabetic, atherosclerosis, retinopathy, neuropathy and nephropathy [6].

Origanum majorana L., is a perennial herb of the mint family (Lamiaceae or Labiatae). Marjoram is used traditionally, as a folk remedy against indigestion, asthma, rheumatism, and headache. Marjoram is used as a spice and its flavour is highly search to consumers worldwide. The spice is valued not only for its flavour but also for its antimicrobial and antioxidant activities [7-9]. Because marjoram has been known to possess medicinal effects, it have been used in pharmaceuticals and the industries of cosmetics [10]. In the present study isolation, structures and anti-AGEs activity of derivatives triterpenes of the oleanane and ursene from the leaves of *Origanum majorana* are described with some comments on the structural requirements for their activity.

Experimental Section

General experimental procedures

IR spectra were obtained on a Perkin-Elmer 1720 FTIR. A Bruker DRX-300 NMR spectrometer, operating at 599.19 MHz for ¹H and 150.86 MHz for ¹³C, using the UXNMR software package, was used for NMR experiments; chemical shifts are expressed in δ (ppm) using TMS as an internal standard. DEPT ¹³C, ID TOCSY, IH- IH DQF-COSY, and HMBC NMR experiments were carried out using the conventional pulse sequences as described in the literature [11]. HREIMS were measured on a JEOL HX 110 mass spectrometer (JEOL, Tokyo, Japan). Precoated TLC silica gel 60 F254 aluminium sheets from Sigma-Aldrich (St. Louis, USA) were used. Column chromatography was carried out on Silica gel 60 (230-400 mesh, Merck Co. New Jersey, USA); solvents used as eluents were from Fermont (California, USA). All other reagents were purchased from Sigma-Aldrich (St. Louis, USA).

Plant material

Fresh leaves of *Origanum majorana* (Lamiaceae) were collected in the county of Amecameca de Juarez (Mexico State). They were identified by the Herbarium of the Metropolitan Autonomous University-Xochimilco. A representative specimen was kept (No. 7419) for further reference.

Isolated of the active constituents of *Origanum majorana*: Air-dried leaves of *Origanum majorana* (9 kg) were ground and extracted successively three times with methanol under reflux (3 h). The filtered samples were combined, and the solvent was evaporated in vacuum to yield the crude residue (874 g). The methanol extract was initially separated by chromatography over a silica gel column (8 X 80 cm, 500 g) and eluted with chloroform. Each fraction (75 ml) was monitored by (thin layer chromatography) TLC; fractions with similar TLC patterns were combined to yield four major fractions (F1-F9). The fractions rich in triterpenes were identified by TLC using the Liebermann-Burchard spray reagent. Each fraction was monitored for its glycation effect in AGEs-BSA formations. Fractions F2, F3 and F5 were rechromatographed over a silica gel column, (2 kg each), fraction F3 was fractionated using as eluent *n*-hexane-chloroform-ethyl ether 0.5:3.5:0.5, to produce six, subfractions (F2-1 to F2-6). However, in the F3 fraction use *n*-hexane-ethyl ether 1:2 to collect nine subfractions (F3-1 to F3-9). F5 was further purified eluted with *n*-hexane-ethyl acetate 3:1 to yield five subfractions (F5-1 to F5-5). Fraction F2-4 was then loaded onto a Sephadex LH-20 column and eluted with CHCl₃-MeOH (2:3); the eluate was then loaded onto a silica gel preparative chromatography and eluted with a gradient system of chloroform-methanol (70:30→0:100). These procedures

yielded pure 1 (40 mg), 7 (45 mg) and 3 (27 mg). The F3-6 mixture was further purified using CHCl₃-acetone (5:1) yielded compounds 6 (38 mg), 9 (20 mg) and 4 (44 mg). Compounds 8 (15 mg), 10 (10 mg) 2 (35 mg) and 12 (28 mg) were purified from fraction F5-5 using a Sephadex LH-20 column chromatography (2.5 X 40 cm, 15 g) using chloroform-methanol gradient system (70:30→0:100). F5-2 yielded 10 (15 mg), 11 (9 mg) and 5 (30 mg) using identical chromatographic conditions. All compounds identified by NMR spectra and comparison of their physical and spectroscopic data to those reported in literature.

3 β ,11 α ,16 β ,21 β -tetrahydroxy-olean-12-en-28 oic acid (1): Amorphous powder, IR (KBr) ν_{\max} (cm⁻¹): 3491 (OH), 1645 (C=C), 1710 (C=O), 1462, 1371, 1250, 1085, 805; HRMS *m/z* 504.3492 (M⁺) calcd for C₃₀H₄₈O₆ 504.3451; ¹H- and ¹³C NMR (CDCl₃) see Table 1.

2 α ,3 β ,21 β ,22 α ,29 α -pentahydroxy-olean-12-en-28-oic acid (2): Amorphous powder, substance, IR (KBr) ν_{\max} (cm⁻¹): 3456 (OH), 1632 (C=C), 1732 (C=O), 1463, 1134, 1014; HRMS *m/z* 520.3472 (M⁺) calcd for C₃₀H₄₈O₇ 520.3400; ¹H- and ¹³C NMR (CDCl₃) see Table 1.

3 β ,15 α ,21 α -trihydroxyolean-olean-12-en-28-oic acid (3): Amorphous powder, IR (KBr) ν_{\max} (cm⁻¹): 3457 (OH), 1732 (CO), 1640 (C=C) 1380; HRMS *m/z* (M⁺) 488.3541 calcd for C₃₀H₄₈O₅ 488.3502; ¹H- and ¹³C NMR (CDCl₃) see Table 1.

2 α ,29 α -diacetoxy,3 β ,23 α -dihydroxy-olean-5,12-dien-28-oic acid (4): Amorphous powder, IR (KBr) ν_{\max} (cm⁻¹): 3461 (OH), 1735 (C=O), 1643 (C=C); HRMS *m/z* 572.3336 (M⁺) calcd for C₃₃H₄₈O₈ 572.3349; ¹H- and ¹³C NMR (CDCl₃) see Table 1.

3 β ,15 α ,23 α ,19 α -tetrahydroxyursan-12-ene-28-oic acid (5): Amorphous powder, IR (KBr) ν_{\max} (cm⁻¹): 3405 (OH), 1732 (C=O), 1668 (C=C); HRMS *m/z* 504.3430 (M⁺) calcd for C₃₀H₄₈O₆ 504.3451; ¹H- and ¹³C NMR (CDCl₃) see Table 2.

2 α ,3 β -diacetoxy-ursan-12,19-diene (6): Amorphous powder, IR (KBr) ν_{\max} (cm⁻¹): 1732 (C=O), 1668 (C=C); HRMS *m/z* 524.3835 (M⁺) calcd for C₃₀H₄₈O₆ 524.3866; ¹H- and ¹³C NMR (CDCl₃) see Table 2.

In vitro glycation of proteins

Determination of glycative product formations by fluorescence spectroscopy: According to the method of Vinson and Howard [12] the reaction mixture, 10 mg/ml of bovine serum albumin (BSA; Sigma, St Louis, MO, USA) in 50 mM phosphate buffer (PH 7.4) with 0.02% sodium azide to prevent bacterial growth, was added to 0.2 M of glucose. The reaction mixture was then mixed with compounds or aminoguanidine (Sigma, St. Louis, MO, USA). After incubating at 37°C for 15 day the fluorescent reaction products were assayed on a spectrofluorometric detector (BIO-TEK, Synergy HT, U.S.A.; Ex: 350 nm, Em: 450 nm).

BSA-methylglyoxal assay

The assay evaluates the middle stage of protein glycation [13]. BSA and methylglyoxal were dissolved in phosphate buffer (100 mM, pH 7.4) to a concentration of 20 mg/ml and 60 mM, respectively. Compounds were dissolved in the same phosphate buffer. 1 ml of the BSA solution was mixed with 1 ml of methylglyoxal solution and 1 ml of the samples. The mixture was incubated at 37°C. Sodium azide (0.2 g/l) was used as an aseptic agent. Phosphate buffer was used as a blank. Aminoguanidine and phloroglucinol were used as positive controls. After seven days of incubation, fluorescence of the samples was measured using an excitation of 340 nm and an emission of 420 nm, respectively.

	1		2		3		4	
	δ_H	δ_C	δ_H	δ_C	δ_H	δ_C	δ_H	δ_C
1	1.02 m, 1.51, m	40.43	2.39 m, 1.34 m	47.54	0.98 m, 1.86 m	38.39	2.31 m, 1.40 m	47.80
2	1.95 m, 2.15 m	30.65	4.18, m	69.64	1.62 m, 1.68, m	25.20	4.47, dd (11.3, 4.9)	78.8
3	3.54, dd, (10.7, 5.3)	79.10	3.69, d (9.4)	83.25	3.23, dd (11.5, 4.7)	78.15	3.41, d (9.5)	81.31
4	-	38.21	-	40.98	-	38.76	-	43.89
5	1.11, dd (15.7, 4.5)	43.28	1.04, m,	56.31	0.84 dd (11.3, 2.4)	54.67	-	145.36
6	1.71, 1.34, m	19.21	1.55 m, 1.40 m	18.54	1.66 m, 1.46 m	18.01	5.29, t (3.5)	121.69
7	1.50, m	34.21	1.56 m, 1.34 m	37.21	1.48 m, 1.30 m	33.21	1.51 m, 1.08,m	33.29
8	-	40.23	-	41.72	-	40.78	-	40.45
9	1.71, m	49.63	-	48.01	1.57, m	47.69	1.56, m	46.59
10	-	-	-	36.57	-	37.21	-	37.12
11	4.28, d, (9.0)	72.67	1.74 m, 1.80 m	23.99	1.86, m	23.91	1.95, m	24.30
12	5.32, d, (3.3)	123.56	5.50, br, s	126.11	5.30, br, s	118.08	5.15, t (3.5)	124.52
13	-	141.56	-	143.36	-	139.64	-	140.03
14	-	43.89	-	43.49	-	42.11	-	41.76
15	3.50, d (13.4), 2.22, t (12.8)	38.16	0.95 m, 1.63 m	26.73	4.19, dd (10.3, 6.1)	73.12	1.62 m, 1.04, m	27.38
16	4.34, dd (11.2, 5.0)	76.59	1.67 m, 1.93 m	28.64	1.52 m, 1.95 m	37.92	1.92, m	23.73
17	-	51.87	-	39.70	-	42.68	-	34.51
18	2.85, dd, (13.7, 3.2)	55.17	2.38, dd (14.3, 4.1)	50.32	2.36, dd (14.1, 4.0)	50.19	2.09 dd (11.2, 3.3)	50.39
19	2.30, t (12.5)	34.37	1.32 m, 2.90 m	46.72	1.94 m, 1.88, m	46.37	-	41.42
20	-	39.19	-	36.49	-	32.45	-	32.40
21	3.47, m	75.52	4.81, d (10)	73.68	4.02, dd (4.0, 10.0)	73.32	1.30 m, 1.36, m	34.39
22	2.47, d (12), 1.29, m	45.37	4.64, d (10)	76.31	2.05 m, 2.08, m	49.52	1.64 m, 1.68, m	28.05
23	0.84, s	29.65	1.23, s	28.65	0.99, s	28.65	3.45, d (11.3), 3.68 d (11.3)	71.23
24	0.82, s	18.64	1.08, s	16.59	0.86, s	16.09	1.03, s	22.78
25	0.91, s	16.73	1.33, s	16.82	1.13, s	16.60	0.93, s	16.42
26	1.07, s	17.43	1.09, s	18.90	1.14, s	18.73	0.85, s	16.89
27	0.98, s	27.41	1.24, s	23.52	1.35, s	23.41	1.17, s	25.19
28	-	178.34	-	179.22	-	180.03	-	181.23
29	1.26, s	32.28	3.62, s	73.73	0.90, s	33.20	-	-
30	1.03, s	23.73	1.25, s	19.73	0.95, s	23.59	1.24, s	24.12
COOMe							2.03 s, 1.98 s	168.70, 172.33

Assignments were confirmed by coupling constant, ^1H - ^1H COSY, NOESY, HMQC, and HMBC analysis in CDCl_3 .

Table 1: ^1H and ^{13}C NMR spectra data for compounds 1-4 (δ in ppm, J in Hz).

Amadorin activity

Amadorin activity was determined using a post-Amadori screening assay [14]. Lysozyme (10 mg/ml) was incubated with 0.5 M ribose in 0.1 M sodium phosphate buffer containing 3 mM sodium azide, pH 7.4 at 37°C for 24 h. Unbound ribose was removed by dialysis against 0.1 M sodium phosphate buffer, pH 7.4 at 4°C for 48 h with 5-6 changes. Following dialysis, the protein concentration was determined using the Bio-Rad standard protein assay kit based on the Bradford dye-binding procedure [15]. Dialysed ribated lysozyme (10 mg/ml) was reincubated with 10 mg/ml of compound or aminoguanidine or pyridoxamine in 0.1 M sodium phosphate buffer containing 3 mM sodium azide, pH 7.4 at 37°C for 15 days.

Determination of N ϵ -(carboxymethyl) Lysine (CML)

BSA was incubated with glucose, ribose and fructose for 4 weeks. N ϵ -CML was determined using an ELISA kit according to the manufacturer's protocol. The absorbance of sample was compared with the CML-BSA standard provided in the assay kit.

Measurement of α -dicarbonyl compounds formation

100 μl of aliquots of glycated material were incubated at room temperature for 1 h with a reaction mixture containing 50 μl of Girard-T stock solution (500 mM) and 850 μl , of sodium formate (500 mM, pH 2.9). Absorbance was measured at 290 nm using a spectrophotometer (UV Mini 1240, Shimadzu, Kyoto, Japan), and glyoxal contents were

calculated using a standard curve for glyoxal. A calibration curve was prepared using 40% glyoxal solution in a similar way [16].

Determination of protein carbonyl content

Protein carbonyl content, a common marker for protein oxidative damage, was measured according to a previous method with minor modifications [17]. Glycated BSA was incubated with 10 mM 2,4-dinitrophenylhydrazine (DNPH) in 2.5 M HCl at room temperature for 1 h. Afterwards, it was precipitated by 20% (w/v) trichloroacetic acid (TCA), left on ice for 5 min, and centrifuged at 10,000 g at 4°C for 10 min. The pellet was washed three times using 1:1 (v/v) ethanol-ethyl acetate mixture. The final pellet was dissolved in 6 M guanidine hydrochloride. The absorbance was recorded at 370 nm. The level of protein carbonyl content was calculated by using an absorption coefficient of 22,000 $\text{M}^{-1}\text{cm}^{-1}$. The results were expressed as nmol carbonyls/mg protein.

Cellular oxidative stress inhibition

Cell-culture and treatment: C2C12 cell purchased from ATCC (Manassas, VA, USA) was cultured in Dulbecco's modified eagle's medium (DMEM) medium supplemented with 10% Fetal calf serum, 100 U/ml penicillin and 100 $\mu\text{g}/\text{ml}$ streptomycin. Cultures were maintained at 37°C in 5% CO_2 incubator. When the cells were about to cover 80% of the flask area, they were disrupted and seeded on 24 well plates. After attaining ~70-80% confluency, the cells were rinsed twice with phosphate buffer saline (PBS) and changed with

	5		6	
	δ_H	δ_C	δ_H	δ_C
1	1.54 m, 1.57 m	38.31	1.10 m, 2.03, m	48.62
2	1.92 m, 1.99 m	27.54	4.56, td (10.3, 10.3, 4.1)	71.27
3	3.59, dd (11.5, 5.3)	73.26	4.34, d (10.3)	80.65
4	-	42.67	-	38.32
5	1.30, m	48.34	1.09, m	55.72
6	1.58, m	18.37	1.55 m, 1.40, m	18.37
7	1.53 m, 1.66, m	33.49	1.52 m, 1.33, m	33.11
8	-	41.26	-	39.64
9	1.88, m	48.38	1.83, m	48.42
10	-	37.62	-	39.86
11	1.97 m, 2.06, m	24.39	2.25 m, 2.07, m	24.67
12	5.22, brt (4.4)	128.73	5.23 t (3.6)	128.54
13	-	141.60	-	139.27
14	-	43.28	-	42.82
15	4.19, dd (11.6, 5.3)	68.41	1.14 m, 1.84, td (13.7, 4.3)	26.89
16	1.27, m, 2.0, t (12.2)	39.10	2.09 td (13.5, 4.3), 0.93 m	23.59
17	-	42.70	-	34.58
18	2.08, d (6.9)	54.79	2.21 d, (6.7)	50.31
19	1.39, m	41.32	1.24, m	40.67
20	0.87, m	48.04	-	134.65
21	3.37, td (11.2, 4.1)	71.79	5.27, d (6.4)	116.43
22	1.24, m, 79, dd (11.2, 4.1)	50.11	1.62 m, 1.33, m	39.55
23	3.49, d (11.2), 3.70 d (11.2)	73.12	0.92, s	28.63
24	1.04, s	21.99	1.02, s	16.74
25	0.92, s	17.05	1.07, m	16.96
26	1.16, s	19.56	0.89, s	28.13
27	1.07, s	13.14	1.0, s	17.84
28	-	180.04	0.82, s	23.47
29	1.01, d (6.1)	18.13	0.89, d (6.4)	24.09
30	0.95, d (6.1)	19.39	1.65, s	23.56
2-COOCH ₃	-	-	2.08, s	172.31, 21.32
3-COOCH ₃	-	-	2.00, s	174.19, 21.59

Assignments were confirmed by coupling constant, ¹H-¹H COSY, NOESY, HMQC, and HMBC analysis in CDCl₃.

Table 2: ¹H and ¹³C NMR spectra data for compounds 5-6 (δ in ppm, *J* in Hz).

medium containing compounds at different concentrations. After 24 h incubation, the cells were washed twice with PBS and 50 μ M H₂O₂ was maintained in individual well for 1 h at 37°C. These cells were detached by trypsin to assay in flow cytometry.

Cytoprotective effect against the oxidative stress induced by H₂O₂ was measured by determining intracellular content of ROS. Intracellular ROS levels were measured employing 2',7'-deoxyribose-dichlorofluorescein-diacetate (DCFH-DA). DCFH-DA is cleaved intracellularly by non-specific esterase and turn to high fluorescent 2,7-dichlorofluorescein (DCF) upon oxidation by ROS, which were analyzed with FACS Aria II Flow Cytometer (BD Bioscience, San Jose, USA). C2C12 cells pretreated with triterpenes were incubated with DCFH-DA at 37°C for 1 h and then read in FACS Aria II.

Statistical analysis

Data are presented as means \pm S.E.M. Statistical comparisons between groups were performed using the Student's t-test. The data were analyzed using the SPSS package (Version 10.0, SPSS, SPSS Inc., Chicago, IL, USA). The values at ^a*p*<0.05 and ^b*p*<0.01 were considered to be statistically significant difference.

Matrix-assisted laser desorption/ionization-time-of-flight-mass spectrometry (MALDI TOF MS)

Glucose (Glu) digests of glycated triterpenes were reconstituted in

trichloroacetic acid (TFA) 0.1%. An aliquot of each sample was mixed (1:1) with α -cyano-4-hydroxycinnamic acid (α -CHCA) matrix solution (5 mg/ml in acrylonitrile 50%/TFA 0.1%) and applied onto 384-well MALDI plates. Instrument was calibrated by adding triterpenes (12.5 ng; 0.5 μ l) to each calibration spot. Peptide mass spectra were obtained with a MALDI-TOF/TOF mass spectrometer (4800 Proteomics Analyzer: Applied Biosystems, Foster City, CA) in the positive ion reflector mode. Spectra were obtained in the mass range between 800 and 7000 Da. Manual interpretation of tandem mass spectra was performed through the Data Explorer software TM ver. 4.4 (Applied Biosystems).

Results and Discussion

The methanol extract of stems of *Origanum majorana*, was fractionated by column chromatography over silica gel and purified by column with sephadex LH-20 and preparative chromatography. In the present study we report the isolation of twelve triterpenes. The compounds were identified by comparison of their physical and spectroscopic data to those reported in literature. The known triterpenes including 28-norlup-20(29)-ene-3 β ,17 β -diol (8, CAS: 202651-66-9) and lupeol (12, CAS: 545-47-1) that were previously isolated from extract of *Origanum majorana* [18]. Lupeol treatment caused decreases in serum glucose, nitric oxide, and glycated haemoglobin, also increase antioxidant levels and serum insulin level [19]. While ursolic acid (10,

CAS: 77-52-1) has been reported that attenuate glycation via mitigating inflammatory and oxidative stress [20]. In addition, this triterpenoid decrease the level of thiobarbituric acid-reactive oxygen species [21]. Furthermore, 3 β ,6 β ,7 β -trihydroxy-20(29)lupine-ene (9) was isolated from *Rhoiptelea chiliantha* [22] and 3 β ,15 α ,dihydroxy-30-norurs-12-ene (11) has been isolated from methanolic extract of *Debregeasia salicifolia* [23]. Oleanolic acid (7, CAS: 508-02-1) was isolated from *Crataegus pinnatifida* showed potent antiglycation activity [24].

Due to the lack of UV chromophore group in the structure of pentacyclic triterpenes, this study was not conducted.

Compound 1 showed strong absorption bands at 3491, 1710 and 1645 cm^{-1} in the IR spectrum indicative of the presence of hydroxyl, carbonyl and double bond groups respectively. The mass spectrum of 1 exhibited a weak molecular ion at m/z 504, which was in agreement with the formula $\text{C}_{30}\text{H}_{48}\text{O}_6$ and seven degrees of unsaturation. This was also supported with analysis of ^1H - and ^{13}C -NMR and the HMQC spectrum, data which were assigned to 1 as shown in Table 1. This compound displayed in DEPT experiments signals for thirty carbons which were distinguished as seven methyls, seven methylenes, eight methines (four oxygenated, three aliphatic, and one vinyl) and eight quaternary carbons (one oxygenated, six aliphatic, and one vinyl). The ^{13}C NMR spectrum showed the presence of a trisubstituted double bond at δ_{C} 123.56 and δ_{C} 141.56 (Table 1) together with the signals of ^1H NMR spectrum for seven singlet methyl groups (δ_{H} 0.84, 0.82, 0.91, 1.07, 0.98, 1.19, 1.03) consistent with an 12-oleanene-28 oic acid carbon skeleton [25]. The presence of four oxygen bearing carbon atom in the molecule were indicated for signals at δ_{H} 79.10, 76.59, 75.52 and 72.67 in the ^{13}C NMR.

A cross peaks of two methyl protons, H3-23 (δ_{H} 0.84) and H3-24 (δ_{H} 0.82), correlated with C-3 (δ_{C} 79.10) carbon showed a hydroxyl group located at C-3 (δ_{C} 79.10). In the ^1H NMR spectrum of 1 the doublet of doublet at δ_{H} 3.54 and doublet at δ_{H} 4.40 were indicative of the deshielded protons attached to the two of the oxygen bearing methine carbons C-3 (δ_{C} 79.10) and C-11 (δ_{C} 72.67), respectively. The oxygenated doublet of doublets at δ_{H} 3.54, which correlated to the

methine carbon at δ_{C} 72.67 in the HETCOR spectrum, was assigned to H-11. The trans diaxial coupling constants $J = 10.7$ and 9.0 Hz for a double doublet (δ_{H} 3.54) and doublet (δ_{H} 4.40) respectively, suggested that both the 3-OH and 11-OH groups should be equatorial. This was also supported on the observed COSY coupling with the olefinic proton doublet resonating at δ_{H} 5.32 (H-12) and the proton doublet absorbing at δ_{H} 1.71 (H-9).

The presence of the hydroxyl group at C-21 was suggested by the ^1H -NMR signal at δ 3.47 (1H, m), the ^{13}C -NMR signal at δ_{H} 75.52 and HMBC correlations of the methyl protons H₃-29 (δ_{H} 1.26) and H₃-30 (δ_{H} 1.03) with C-18 (δ_{C} 55.17), C-19 (δ_{C} 34.37), C-21 (δ_{C} 75.52) and C-22 (δ_{C} 45.37) carbons; H-22 α (δ_{H} 2.42) and H-22 β (δ_{H} 1.26) with C-21 (δ_{H} 75.52) carbon. The β configuration of the hydroxyl group at H-21 in the NOESY spectrum, was identified from the correlations H-21 (δ_{H} 3.47) with H-29 (δ_{H} 1.26).

In the HMBC spectrum, proton H-22 α (δ_{H} 2.47) correlated with C-16 (δ_{C} 76.59) carbon, which revealed a hydroxyl group located at C-16 (δ_{C} 76.59). This suggestion could be confirmed by the correlations as H-15 (δ_{H} 3.50 and 2.22) correlated with C-16 (δ_{C} 76.59) and C-27 (δ_{H} 27.41) carbons, respectively. β configuration of the hydroxyl group at C-16 was identified from the correlation between H-16 (δ_{H} 4.34) and H-27 (δ_{H} 0.98). The other oxygenated carbon, which appeared at δ_{C} 181.34 as a quaternary carbon in the DEPT spectrum, was attributed to C-28 as a carboxylic acid group. The structure of compound 1 being, 3 β ,11 α ,16 β ,21 β -tetrahydroxy- olean-12-en-28 oic acid (Figure 1).

Compound 2 was isolated as amorphous powder and showed positive Molish and Liebermann-Burchard reaction tests. The molecular formula was established as $\text{C}_{30}\text{H}_{48}\text{O}_7$ according to HRESIMS, m/z 520.3472 [M]⁺ (calcd. for $\text{C}_{30}\text{H}_{48}\text{O}_7$ 520.3400). The IR spectrum contained carbonyl (1732 cm^{-1}), hydroxyl (3456 cm^{-1}) and a typical absorption of a double bond (1632 cm^{-1}) function. DEPT, HMQC and ^{13}C NMR spectra displayed thirty carbon atoms assigned to six methyl groups, eight methylenes including one hydroxy methyl, eight methynes including four hydroxyl groups and one olefinic group,

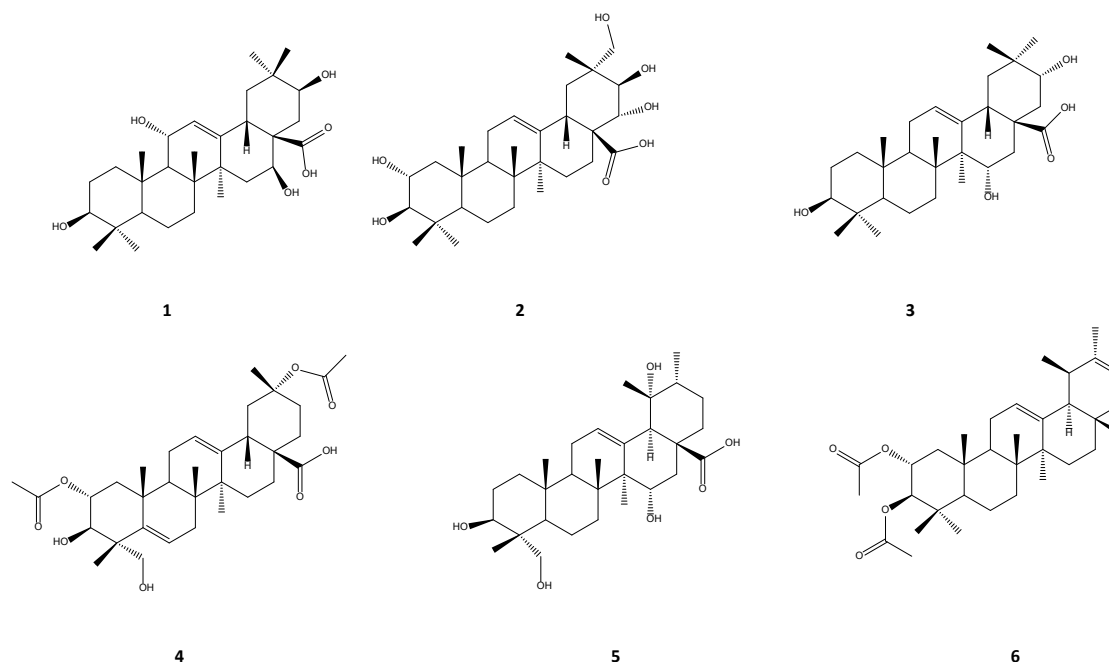


Figure 1: Triterpenoids isolated from *Origanum majorana*.

eight quaternary carbon including one carboxyl group, with a degree of unsaturation of seven. ^1H NMR spectrum of 2 (Table 1) showed signals for six tertiary methyl groups at δ_{H} 1.23 (3H, s), δ_{H} 1.08 (3H, s), δ_{H} 1.33 (3H, s), δ_{H} 1.09 (3H, s), δ_{H} 1.24 (3H, s), 1.25 (3H, s). Thus, 2 was deduced to be a oleanane derivative. HMBC experiment showed the correlation of H_3 -23 (δ_{H} 1.23) and H_3 -24 (δ_{H} 1.08), with C-3 (δ_{C} 83.25) which have a hydroxyl group. The carbinol group of the C-3 (δ_{C} 83.25) is 7 ppm downfield shift compared to other analogues [26], indicated that C-2 have an oxygenated carbon. In the HMBC spectrum, correlation signals from δ_{H} 3.69 (H-3) to δ_{C} 69.64 (C-2), δ_{C} 40.98 (C-4), δ_{C} 28.65 (C-23) and δ_{C} 16.59 (C-24) were observed, supported the linked of the two hydroxyl groups at C-2 and C-3. In NOESY spectrum showed correlations of H-3 (δ_{H} 3.69) with Me-23 (δ_{H} 1.23) of H-2 (δ_{H} 4.19) with Me-24 (δ_{H} 1.08) and Me-25 (δ_{H} 1.33) together with the large proton spin-coupling constant of H-3 ($^3J_{2,3} = 9.4$ Hz) indicated the α - and β -orientation of the hydroxyl groups at C-2 and C-3, respectively [27]. AB system signal, for one hydroxymethyl group in the ^1H NMR spectrum at δ_{H} 3.62 (2H, s) together with HMBC spectrum showed correlations from δ_{H} 3.62 (H₂-29) to C-19 (δ_{C} 46.72), C-20 (δ_{C} 36.49), and C-30 (δ_{C} 19.73), supported the linked of the hydroxyl group at C-29 but not at C-30. The α -orientation of hydroxymethyl group and the β -axial configuration of H-18 was suggested by NOE correlations of H-18 β (δ_{H} 2.38) with H-12 (δ_{H} 5.50) and H-30 (δ_{H} 1.25) and the coupling constant of H-18 β , (dd $J = 14.3, 4.1$ Hz). HMBC correlations from δ_{H} 5.50 (H-12) to C-9 (δ_{C} 48.01), C-14 (δ_{C} 43.49) and C-18 (δ_{C} 43.49) indicated the double bond at C-12(13). The signal H-16 (δ_{H} 1.93) and H-18 (δ_{H} 2.38), correlated with carbonyl signal at δ_{C} 179.22 suggested that the carboxyl group were connected to C-17.

The location of the other two hydroxy groups was carried out by ^1H - ^1H COSY spectrum indicated correlations of H-18 (δ_{H} 2.38) to H-19 (δ_{H} 2.90, 1.32) and H-21 (δ_{H} 4.81) to H-22 (δ_{H} 4.64) [28]. In the NOESY spectrum NOE correlations between H-18 (δ_{H} 2.38) to H-30 (δ_{H} 1.25) and H-18 (δ_{H} 2.38) to H-22 (δ_{H} 4.64) supported the α -orientation of the hydroxyl groups linked to C-22 (δ_{C} 76.31) and C-29 (δ_{C} 73.73). Moreover, the β -orientation of the hydroxyl groups linked to C-21 was confirm by large values of the proton coupling constant between H-21 and H-22 ($J = 10$ Hz) [29]. However, HMBC spectrum showed correlations of H-18 (δ_{H} 2.38) with C-20 (δ_{C} 36.49); H-19 (δ_{H} 2.90, 1.32) with C-21 (δ_{C} 73.68), C-29 (δ_{C} 73.73), and C-30 (δ_{C} 19.73); H-21 (δ_{H} 4.81), with C-29 (δ_{C} 73.73), and C-30 (δ_{C} 19.73); H-22 (δ_{H} 4.64), with C-20 (δ_{C} 36.49) confirm the location of the three hydroxy groups in E ring. On the basis of these results the structure of 2 was determined as 2 α ,3 β ,21 β ,22 α ,29 α -pentahydroxy olean-12-en-28-oic acid (Figure 1).

Compound 3 was isolated as amorphous powder. Its molecular formula was established as $\text{C}_{31}\text{H}_{50}\text{O}_5$ on the basis of HRESI-MS, m/z 502.3681 [M]⁺ (calcd. for $\text{C}_{31}\text{H}_{50}\text{O}_5$, 502.3658). The IR spectrum showed typical absorptions bands for a double bond (1640 cm^{-1}), carbonyl (1732 cm^{-1}), and hydroxyl (3457 cm^{-1}) groups. The ^{13}C - and DEPT spectral data displayed 31 carbon resonances (Table 1) including eight methyl groups, eight methylenes, seven methynes and eight quaternary carbon. HMBC spectrum showed correlations of H-18, and H-19 with olefinic quaternary carbon (δ_{C} 139.64, C-13). The double bond was located between C-12 and C-13. Confirming the location of the double bond with the correlations of H-18 and H-9 correlations to the olefinic methine (δ_{C} 118.08, C-12). The location of the C-3 hydroxy group was determined by HMBC experiments in which H-3 exhibited 2J correlations with C-2 (δ_{C} 25.20) and C-4 (δ_{C} 38.76) and 3J correlations with C-1 (δ_{C} 33.72), C-5 (δ_{C} 54.67) and C-24 (δ_{C} 16.59). In addition, showed correlations between of H-23 (δ_{H} 0.99) and H-24 (δ_{H} 0.86) with C-3 (δ_{C} 78.15) confirmed the location of hydroxyl group at C-3. The correlations between H-15 (δ_{H} 4.19) to C-8 (δ_{C} 40.78), C-17 (δ_{C} 42.68)

and C-27 (δ_{C} 23.41), C-15 (δ_{C} 73.12) with H₂-16 (δ_{H} 1.52/1.95) and H₃-27 (δ_{H} 1.35) indicated that the second hydroxy group was located at C-15 [30]. The configurations of both hydroxy groups at C-3 and C-15 were assigned as β and α -orientations respectively, due to the trans-diaxial coupling constants of H-3 ($J = 11.5$ Hz) and H-15 ($J = 10.3$ Hz). In NOESY experiments correlations between signals at δ_{H} 3.23 (H-3), δ_{H} 0.84 (H-5) and those at δ_{H} 4.19 (H-15) and δ_{H} 1.14 (H-26) confirmed the β - and α -orientations of H-3 and H-15 respectively.

The location of the remaining hydroxyl group was determine to be at C-21 on the basis of HMBC correlation of H-22 (δ_{H} 2.05/2.08) to C-18 (δ_{C} 50.19), C-20 (δ_{C} 32.45) and C-21 (δ_{C} 73.32); H-29 (δ_{H} 1.94/1.88) to C-21 (δ_{C} 73.32). The relative configuration of hydroxyl group was determined as α -equatorial orientation according on the coupling constant of H-21 ($J = 4.0, 10$ Hz) [31]. Therefore compound 3 was concluded to be 3 β ,15 α ,21 α -trihydroxyolean-olean-12-en-28-oic acid (Figure 1).

Compound 4 was obtained as amorphous powder. The molecular formula was $\text{C}_{33}\text{H}_{48}\text{O}_8$ on the basis of HRESI-MS. The IR spectrum showed the presence of hydroxyl (3461 cm^{-1}), carbonyl (1735 cm^{-1}), and double bond (1643 cm^{-1}) groups absorption bands. ^{13}C NMR and DEPT spectra revealed thirty-three signals assigned to seven methyl groups, nine methylenes, six methynes and eleven quaternary carbon, with a degree of unsaturation of ten. The ^1H NMR spectrum of 4 showed signal attributable to two downfield protons at δ_{H} 5.29 and δ_{H} 5.15 assigned to H-6 and H-12 respectively, the sharp of three proton singlets at δ_{H} 2.03 and δ_{H} 1.98 revealed the presence of two acetyl groups and five tertiary methyl group at 0.85, 0.93, 1.03, 1.17 and 1.24. The H₃-30 methyl appeared as a three proton singlet at 1.24, corresponding of the oleanane-type triterpene skeleton. Also was observed an acetoxy group at δ_{H} 2.03 (3H, s), a methyne proton attached an acetoxy group at δ_{H} 4.47. HMBC correlations of the proton signals at H-3 (δ_{H} 3.41) with δ_{C} 47.80 (C-1), δ_{C} 43.89 (C-4), δ_{C} 71.23 (C-23), δ_{C} 22.78 (C-24), and H-23 (δ_{H} 3.45/3.68) with δ_{C} 81.31 (C-3), δ_{C} 43.89 (C-4), and δ_{C} 145.36 (C-5) supported the location of hydroxyl groups at C-3 and C-24 respectively. Based on NOE correlations between H-3 α and H-23 and coupling constant of H-3 ($J = 9.5$ Hz) hydroxyl group was assigned β -equatorial and the hydroxymethyl group at C-23 as α -orientation. The signal H-16 (δ_{H} 1.93) and H-18 (δ_{H} 3.38), correlated with carbonyl signal at δ_{C} 179.22 suggested that the carboxyl group were connected to C-17. The position of acyl groups at C-2 was clarified by HMBC experiment. Long range correlations were observed between the proton of C-2 and the carbonyl carbon of the acetyl group. In HMBC spectrum the C-30 methyl protons displayed correlations with carbonyl of the C-29 and the methylene carbons 19 and 21. The other acetyl group was assigned at C-20 by NOE correlations with H-30 to H-18; H-18 to H-22 which suggested the α -orientation of the 29-COOMe at C-20. The double bonds were located at C-5/C6 and C-12/C-13 by HMBC correlations of H-23 and H-24 to C-5; H-23 to C-6; H-24 to C-6; H-25 to C-5; H-27 to C-13. Consequently compound 4 was established as 2 α ,29 α -diacetoxy, 3 β ,23 α -dihydroxy- olean-5,12-dien-28-oic acid (Figure 1).

Compound 5 was isolated as amorphous powder and showed positive Molish and Liebermann-Burchard reaction tests. The molecular formula was established as $\text{C}_{30}\text{H}_{48}\text{O}_6$ according to HRESI-MS, m/z 504.3630 [M]⁺ (calcd. for $\text{C}_{30}\text{H}_{48}\text{O}_6$, 504.3451) indicating seven degrees of unsaturation. The IR spectrum contained typical absorptions of hydroxyl (3405 cm^{-1}) and carbonyl (1732 cm^{-1}) groups, and a double bond (1668 cm^{-1}) function. The ^{13}C - and DEPT spectral data indicated the presence of thirty carbons assigned to six methyl groups, eight methylenes including one hydroxy methyl, nine methynes including one olefinic and three hydroxyl groups, seven quaternary carbon including one carbonyl. These data are in agreement with the molecular formula

indicated that 5 was ascribed to be derivate of ursane triterpenoids. The location of the C-3 hydroxy group, C-23 hydroxy group, C-28 acid group and C-12 double bond function were determined via an HMBC and NOESY experiments indicated the similarity with those of 4 (Table 1) showed a common 3 β ,23 α -diol- urs-12-ene-28 oic acid nucleus for the triterpene. The HMBC correlations between H-15 (δ_H 4.19) with C-8 (δ_C 41.26), C-17 (δ_C 42.70) and C-27 (δ_C 13.14); H₂-16 (δ_H 1.57/2.0) with H₃-27 (δ_H 1.07) and C-15 (δ_C 68.41) indicated that the second hydroxy group was located at C-15. The configurations of the hydroxy groups at C-3 and C-15 were assigned as β and α -orientations respectively, due to the trans-diaxial coupling constants of H-3 ($J=11.5$ Hz) and H-15 ($J=10.6$ Hz). Furthermore, in the NOESY experiments correlations were observed between δ_H 3.59 (H-3), δ_H 1.30 (H-5) and those at δ_H 4.19 (H-15) and δ_H 1.16 (H₃,26) confirmed the α - and β -orientations of H-3 and H-15 respectively (Table 2). Therefore compound 5 was concluded to be 3 β ,15 α ,23 α ,19 α -tetrahydroxyursan-12-ene-28-oic acid (Figure 1).

Triterpene 6 was isolated as a colorless solid. The molecular formula C₃₄H₅₂O₄ was established by its ¹³C NMR and MS data, contained double bond, and acetoxy groups attributable to the IR absorption bands at 1606, and 1732 cm⁻¹ respectively. The ¹H NMR spectrum confirmed that is a triterpene skeleton with an ursolic acid type with a double bond at C-12-C-13, and two carboxyl group at δ_C 172.31, and δ_C 174.19. The large coupling constant ($J_{2,3}$) of 10.3 Hz is typical to an antiperiplanar (axial-axial) relationship between H-2 and H-3 (Table 2) suggested the α - and β - orientation of acetyl groups at C-2 and C-3 respectively. The NOE correlations of H-2 (δ_H 4.56) with H-24 (δ_H 1.02) and H-25 (δ_H 1.07); H-3 (δ_H 4.34) with H-23 (δ_H 0.92) supported these positions. The ¹H NMR spectrum of 6 exhibited signals for a methine proton at δ_H 2.21 (1H, d, $J=6.7$ Hz, H-18 α), and the presence of one olefinic double bond at δ_H/δ_C 5.23/128.54 (H-12/C-12) and δ_C 139.27 (C-13) an additional olefinic double bond at δ_H/δ_C 5.27/116.43 (H-21/C-21) and δ_C 134.65 (C-20) and an olefinic methyl group at δ_H/δ_C 1.65/23.56 (H₃-30/C-30). The position of the double bond was established to be at C-20/C-21 based on the HMBC correlations of H₃29/C-20, H-21/C-19, H-21/C-20, H₃30/C-20, H-21/C-30 and H₃30/C-21. Thus, the structure of compound 6 was elucidated to be 2 α ,3 β - diacetoxy-ursan-12,19-diene (Figure 1).

In this study triterpenes 1-6 were evaluated for their ability to retard glycation reaction between glucose and albumin (Table 1). Among them, triterpenes 2 and 1 exhibited the most potential inhibitory activity against AGEs formation, with IC₅₀ values of 39 μ M, 26 μ M and 82 μ M respectively. Compounds 3, 4 and 5 also showed stronger inhibitory activities (IC₅₀ values ranging from 128 to 200 μ M) than a well known positive control, aminoguanidine (IC₅₀ value of 959 μ M). However 6 showed very little activity (IC₅₀ value of 1301) than that produced by the AG.

The inhibitory effects of triterpenes on methylglyoxal-mediated protein glycation were evaluated. Compounds 2, 1, and 3 exhibited significant inhibition, and their IC₅₀ values were 201, 188, and 224 μ M respectively, compared to AG (IC₅₀, 335 μ M). compounds 4 and 5 showed strong inhibition with IC₅₀ values of 300 and 242 μ M respectively (Table 3). Methylglyoxal is a dicarbonyl intermediates as mediators of advanced glycation endproduct formation and are known to react with arginine, cysteine and lysine residues in proteins to form glycosylamine protein crosslinks [32,33].

A G. K. peptide containing a lysine residue was incubated with D-ribose for 24 h. This model system was used to evaluate the inhibitory effects of triterpenes on protein cross-linking. As shown in

Table 3, compound 2 exhibited substantial anti-cross-linking activities. At a concentration of 10 mM, the inhibitory effect of compound 2 and pyridoxamine was 78% and 64%, respectively (Table 3).

For a period of 24 h exposure of lysozyme to ribose produced glycated protein rich in Amadori but not advanced glycation adducts [32]. Lysozyme is widely used for investigation of glycation-induced crosslinking. Triterpenes inhibit cross-linked advanced glycation endproducts and also have Amadorin activity to concentration of 50 μ g/ml (Table 3). Pyridoxamine, used as positive control may inhibit at multiple stages of advanced glycation endproduct formation. This contrasts with other inhibitors, such as aminoguanidine which has no Amadorin activity [34].

These results indicated that for each stage of protein glycation compound 2 had the most potent inhibitory effect of all the compounds isolated from *O. majorana*. These observations suggested that the compounds can potentially inhibit the glycooxidative modification of proteins.

N^ε-CML, is a glyco-oxidation product which is not fluorescent and not reactive, is produced from the oxidative degradation of Amadori products [32]. CML is an indicator of the advanced stages of the Maillard reaction. Table 4 shows the effect of 1-6 on N^ε-CML level in glycated BSA after 4 weeks of incubation. Triterpenes 1-5 significantly ($p<0.05$) reduced the concentration of N^ε-CML level in BSA + Glucose (39.53%, 51.16%, 34.88, 25.58%, and 30.23%), Fructose-glycated BSA (44.44%, 50.61%, 38.27%, 22.22% and 28.39%) and BSA + Ribose (43.44%,

Inducer	Treatment	Inhibitory effects IC ₅₀ value; μ M
Glucose	Methanol extract	656 \pm 12.56
	Aminoguanidine	959 \pm 32.65
	Phloroglucinol	710 \pm 7.59
	1	82 \pm 17.64
	2	39 \pm 11.53
	3	128 \pm 22.17
	4	200 \pm 21.06
Methylglyoxal	Methanol extract	196 \pm 28.21
	Aminoguanidine	335 \pm 15.34
	Phloroglucinol	205 \pm 17.63
	1	201 \pm 28.31
	2	188 \pm 18.76
	3	224 \pm 15.83
	4	300 \pm 30.21
Lysozyme/ribose	Methanol extract	70.5%
	Aminoguanidine	0%
	Pyridoxamine	64%
	1	73.2%
	2	77.9%
	3	66.5%
	4	50.3%
5	60.5%	
6	11.4%	

Data are mean \pm standard deviation of triplicate tests. The concentration of triterpenoids used in the AGEs formation methods were of 20, 30, 50, 100, 200, 300, 500, 750, 1000, 1200, and 1300 μ M. However, in lysozyme/ribose method was used 10 mM.

Table 3: The inhibitory effects of triterpenes 1-6 and aminoguanidine on the formation of advanced glycation end products (AGEs), *in vitro* induced by glucose, methylglyoxal and ribose.

47.77%, 36.70%, 33.70% and 35.01%). The percentage inhibition of triterpenes 1-5 on N^c-CML concentration were lower than percentage inhibition of AG in BSA + Glucose, BSA + Fructose, and BSA + Ribose.

The effect of triterpenes 1-5 at concentration of 1 mM on protein carbonyl content (PCO) in BSA incubated with ribose, fructose and glucose is shown in Table 4. The results indicated a significant reduction of PCO content level in BSA+Glu (47.78%-64.60%), BSA+Rib (38.08%-53.49%) and BSA+Fruc (47.01%-65.57%). In addition, BSA in the presence of AG also to concentration of 1 mM significantly inhibited PCO (47.34% in BSA+Glu, in 31.52% BSA+Rib and 40.39% in BSA+Fruc). Comparing with the percent reduction in PCO of 1-5 were more effective than AG at the same concentration.

The ability of triterpenes 1-5 to inhibit α -dicarbonyl compounds formation is showed in Table 5. The effect of 1-5 on glyoxal content showed all isolated have less inhibitory effect than that produced by the quercetin used as positive standard. Among the isolated compounds 2 had stronger inhibition activity.

The ability of the triterpenes 1-5 to decrease the oxidative stress in cells was evaluated by intracellular oxidative stress induced by H₂O₂ in

C2C12 cells. The oxidative stress reduction is showed in Table 5. The capacity of triterpenes (50 μ g/ml) to reduce the oxidative stress was compared with that of ascorbic acid (25 μ g/ml). The triterpenes 1-5 were less potent than ascorbic acid.

Glycation of triterpenes was monitored by MALDI-MS through the increase in the molecular weight of protein as a result of glucose adducts formation with the honnone. Figure 2 shows the typical mass spectra of positive (a) and mass spectra of BSA. In Figure 3, we can observe a typical spectrum of glycated protein where glycation of the protein was performed by incubation with 220 mM glucose for 30 d at 37°C in the absence of reducing conditions and glycated protein with 1 (a). The major peak at *m/z* 67925.163 corresponds to native BSA whereas the second peak at *m/z* 3999.656 corresponds to a diglycated form of BSA. A third minor peak at *m/z* 5397.765 is also observable and should correspond to a monoglycated form. Figure 3b, shows a different mass profile, especially in terms of relative abundance of each specie. There are two additional peaks in the spectrum besides the peak corresponding to native BSA. The major peak, at *m/z* of 5397.765, is the protonated

Concentration (50 μ g/ml)	Inhibition of CML (ng/ml)	Protein carbonyl content (nmol/mg/protein)
BSA	1.9 \pm 0.4	0.29 \pm 0.008
BSA + Glucose (Glu)	4.3 \pm 1.2 ^a	2.26 \pm 0.034 ^a
BSA + Glucose + 1	2.6 \pm 0.8 ^b	0.88 \pm 0.011 ^b
BSA + Glucose + 2	2.1 \pm 0.7 ^b	0.80 \pm 0.037 ^b
BSA + Glucose + 3	2.8 \pm 1.0 ^b	0.95 \pm 0.043 ^b
BSA + Glucose + 4	3.2 \pm 1.3 ^b	1.18 \pm 0.016 ^b
BSA + Glucose + 5	3.0 \pm 0.9 ^b	1.07 \pm 0.039 ^b
BSA + Glucose + 6	4.0 \pm 1.5	2.03 \pm 0.039
BSA + Glucose + AG	2.3 \pm 0.7 ^b	1.19 \pm 0.079 ^b
BSA + Fructose (Fruc)	8.1 \pm 2.1 ^a	3.02 \pm 0.082 ^a
BSA + Fructose + 1	4.5 \pm 1.2 ^b	1.15 \pm 0.021 ^b
BSA + Fructose + 2	4.0 \pm 1.9 ^b	1.10 \pm 0.017 ^b
BSA + Fructose + 3	5.0 \pm 0.8 ^b	1.31 \pm 0.045 ^b
BSA + Fructose + 4	6.3 \pm 0.6 ^b	1.60 \pm 0.048 ^b
BSA + Fructose + 5	5.8 \pm 0.7 ^b	1.49 \pm 0.050 ^b
BSA + Fructose + 6	7.8 \pm 0.7	2.81 \pm 0.093
BSA+ Fructose + AG	4.1 \pm 1.8 ^b	1.80 \pm 0.045 ^b
BSA + Ribose (Rib)	53.4 \pm 3.17 ^a	7.01 \pm 0.034 ^a
BSA + Ribose + 1	30.2 \pm 6.19 ^b	3.88 \pm 0.059 ^b
BSA + Ribose + 2	27.89 \pm 5.12 ^b	3.75 \pm 0.087 ^b
BSA + Ribose + 3	33.8 \pm 4.19 ^b	4.05 \pm 0.073 ^b
BSA + Ribose + 4	35.4 \pm 6.11 ^b	4.34 \pm 0.037 ^b
BSA + Ribose + 5	34.7 \pm 3.93 ^b	4.21 \pm 0.026 ^b
BSA + Ribose + 6	50.9 \pm 5.17	6.77 \pm 0.062 ^b
BSA+ Ribose + AG	34.5 \pm 3.76 ^b	4.80 \pm 0.078 ^b

Data are mean \pm standard deviation (n = 3) ^a*p*<0.05 when compared to BSA ; ^b*p*<0.05 when compared to BSA + Glu, BSA + Fruc and BSA + Rib.

Table 4: Effect of triterpenes 1-6 on non-fluorescence N^c-CML level and protein carbonyl content.

Groups	% DCF fluorescence	α -dicarbonyl compounds (IC ₅₀ μ g/ml)
Blank	7.12	-
Control	68.34	-
Ascorbic acid	16.38	-
Quercetin	-	62.5 \pm 13.19
1	40.23	124.8 \pm 8.56
2	34.27	105.7 \pm 9.28
3	45.67	140.2 \pm 10.38
4	51.30	173.0 \pm 13.78
5	48.47	160.3 \pm 12.26

Values represents mean \pm SD (n = 3).

Table 5: Reduction activity of triterpenes 1-5 on cellular oxidation stress and α -dicarbonyl compounds.

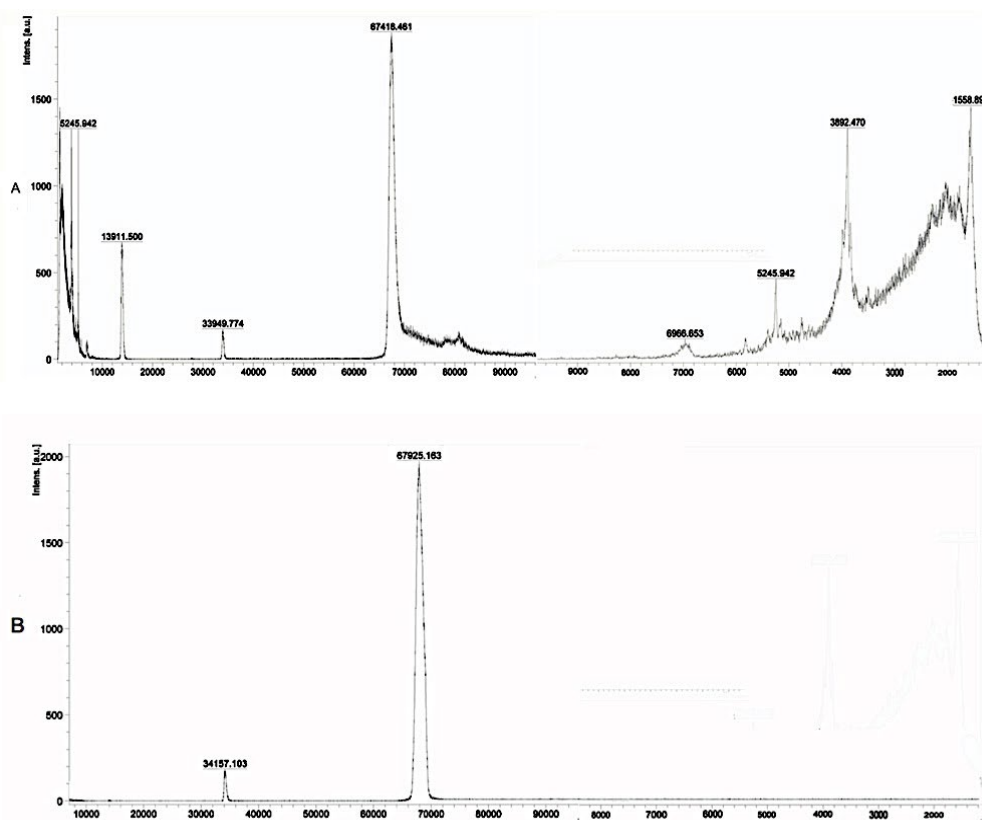


Figure 2: Positive ion MALDI linear TOF MS, with the standard (sinapic acid) SEM detector (a) and BSA (b).

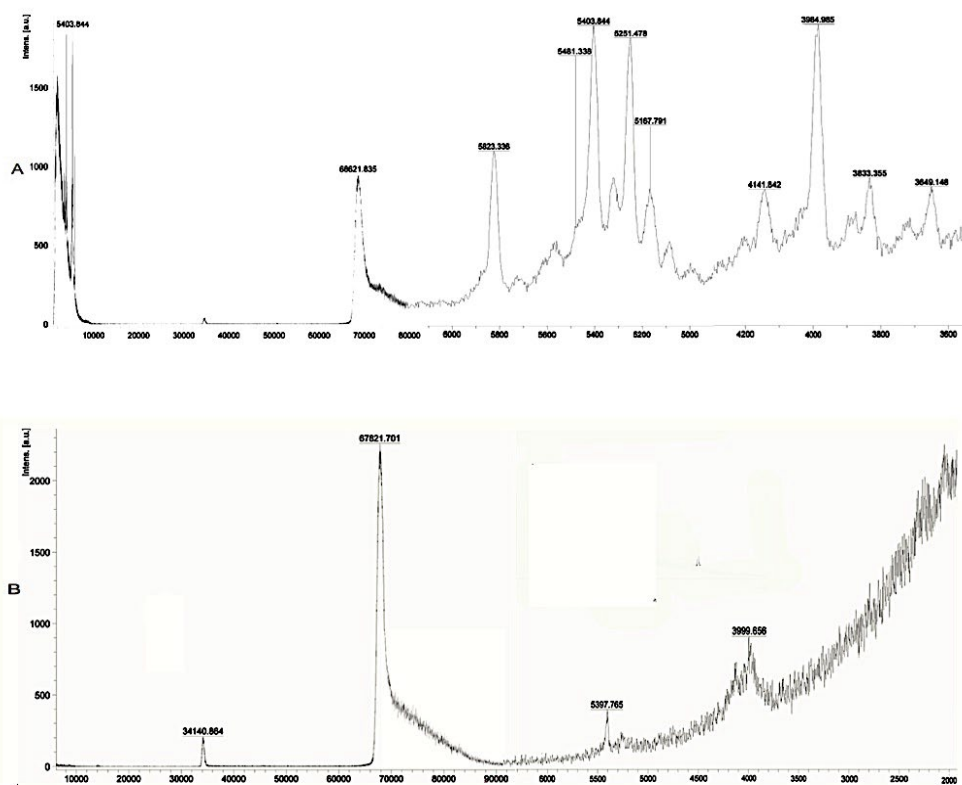


Figure 3: Chromatogram (a) show mono- di- and tri- adducts of BSA+ glucose after incubation 15 days at 37°C. MALDI TOF MS spectra (b) of monomero-glucose, dimero-glucose and trimero-glucose adducts of 2 α ,3 β ,21 β ,22 α ,29 α -pentahydroxy-olean-12-en-28-oic acid.

monoglycated form. The other peaks at m/z 3999.656 correspond to the protonated diglycated and triglycated forms, respectively.

In all screening compound 2 displayed the most potent activity whereas compounds 1, 3, 5 and 4 gave significantly activity, instead compound 6 has much weaker activity considered inactive. This results suggested that the loss of the hydroxyl groups caused a significant loss of activity, revealing also the importance of the carboxyl group since no activity was observed in compound 6 which lacks this group. In general, the most active derivatives were oleanane followed by urseno. Interestingly, acetyl groups greatly diminished activity. Structural variations involving the hydroxyl groups substituted rings resulted in considerable improvement in inhibited AGEs.

In conclusion, according to the data obtained in this study *Origanum majorana* leaves extract contain various triterpenoids which showed excellent effect anti-glycation and they are effective inhibiting cellular oxidations. In particular, $2\alpha,3\beta,21\beta,22\alpha,29\alpha$ -pentahydroxy-olean-12-en-28-oic acid (2) displaying potent activity when compared to aminoguanidine a known glycation agent.

References

- Matafome P, Sena C, Seica R (2013) Methylglyoxal, obesity, and diabetes. *Endocrine* 43: 472-484.
- Singh RA, Barden T, Mori L (2001) Advanced glycation end-products: A review. *Diabetologia* 44: 129-146.
- Meerwaldt RT, Links C, Zeebregts R, Hillebrands JL, Smit A (2008) The clinical relevance of assessing advanced glycation endproducts accumulation in diabetes. *Cardiovas Diabetol* 7: 29-32.
- Kaneto H, Katakami N, Matsuhisa M, Matsuo TA (2010) Role of reactive oxygen species in the progression of type 2 diabetes and atherosclerosis. *Mediators Inflamm* 2010: 453892.
- Giacco F, Brownlee M (2010) Oxidative stress and diabetic complications. *Circ Res* 107: 1058-1070.
- Ahmed N (2005) Advanced glycation endproducts--role in pathology of diabetic complications. *Diabetes Res Clin Pract* 67: 3-21.
- Deans SG, Svoboda KP (1990) The antimicrobial properties of marjoram (*Origanum majorana* L.) volatile oil. *Flavour Fragrance J* 15: 187-190.
- Jun WJ, Han B, Yu K, Kim Y, Chang I, et al. (2001) Antioxidant effects of *Origanum majorana* L. on superoxide anion radicals. *Food Chem* 75: 439-444.
- Lagouri V, Boskou D (1996) Nutrient antioxidants in oregano. *Int J Food Sci Nutr* 47: 493-497.
- Vera RR, Chane M J (1999) Chemical composition of the essential oil of marjoram (*Origanum majorana* L.) from Reunion Island. *Food Chem* 66: 143-145.
- Nolis P, Parella T (2005) Spin-edited 2D HSQC-TOCSY experiments for the measurement of homonuclear and heteronuclear coupling constants: application to carbohydrates and peptides. *J Magn Reson* 176: 15-26.
- Vinson JA, Howard TB (1996) Inhibition of protein glycation and advanced glycation end products by ascorbic acid and other vitamins and nutrients. *Nutrition Biochem* 7: 659-663.
- Khalifah RG, Baynes JW, Hudson BG (1999) Amadorins: novel post-Amadori inhibitors of advanced glycation reactions. *Biochem Biophys Res Commun* 257: 251-258.
- Yin MC, Huang SW, Chan KC (2002) Non-enzymatic antioxidant activity of four organosulfur compounds derived from garlic. *J Agric Food Chem* 50: 143-6147.
- Bradford MA (1976) Rapid and sensitive method for the quantitation of microgram quantities of protein utilizing the principle of protein-dye binding. *Anal Biochem* 72: 248-254.
- Mitchel REJ, Bimboim HC (1977) The use of Girard-T reagent in a rapid and sensitive method for measuring glyoxal and certain other α -dicarbonyl compounds. *Anal Biochem* 81: 47-56.
- Levine RL, Garland D, Oliver CN, Amici A, Climent I, et al. (1990) Determination of carbonyl content in oxidatively modified proteins. *Methods Enzymol* 186: 464-478.
- Nunez MJ, Reyes CP, Jimenez IA, Moujir L, Bazzocchi IL (2005) Lupane triterpenoids from *Maytenus* species. *J Nat Prod* 68: 1018-1021.
- Yin M (2012) Anti-glycative potential of triterpenes: A minireview. *Biomedical* 1: 2-9.
- Gupta RI, Sharma AK, Sharma MC, Dobhal MP, Gupta RS (2012) Evaluation of antidiabetic and antioxidant potential of lupeol in experimental hyperglycaemia. *Nat Prod Res* 26: 1125-1129.
- Fourie TG, Matthee E, Snyckers FO (1989) A pentacyclic triterpene acid, with anti-ulcer properties, from *Cussonia natalensis*. *Phytochemistry* 28: 2851-853.
- Zhi-Hong J, Takashi T, Isao K (1995) A lupane triterpene and two triterpene caffeates from *Rhoiptelea chiliantha*. *Phytochemistry* 40: 1223-1226.
- Akbar E, Riaz M, Malik A (2001) Ursene type nortriterpene from *Debregeasia salicifolia*. *Fitoterapia* 72: 382-385.
- Chowdhury SS, Islam MN, Jung HA, Choi JS (2014) In vitro antidiabetic potential of the fruits of *Crataegus pinnatifida*. *Res Pharm Sci* 9: 11-22.
- Nick A, Wright AD, Sticher O, Rali T (1994) Antibacterial triterpenoid acids from *Dillenia papuana*. *J Nat Prod* 57: 1245-1250.
- Lavaud C, Crublet ML, Pouny L, Litaudon M, Sevenet T (2011) Triterpenoid saponins from the stems of *Elatostachys apetala*. *Phytochemistry* 57: 469-478.
- Cheng SY, Wang CM, Hsu YM, Huang TJ, Chou SC, et al. (2011) Oleanane-type triterpenoids from the leaves and twigs of *Fatsia polycarpa*. *J Nat Prod* 74: 1744-1750.
- Mimaki Y, Kuroda M, Yokosuka A, Harada H, Fukushima M, et al. (2003) Triterpenes and triterpene saponins from the stems of *Akebia trifoliata*. *Chem Pharm Bull (Tokyo)* 51: 960-965.
- Zhang XY, Huo LR, Liu LF, Xu ZQ, Wang WJ (2011) Chemical constituents from leaves of *Gymmema sylvestri*. *Chin Traditional Herbal Drugs* 42: 866-869.
- Zhang Z, Koike K, Jia K, Nikaido T, Guo D, Zheng J (1999) New saponins from the seeds of *Aesculus chinensis*. *Chem Pharm Bull* 47: 1515-1520.
- Caceres-Castillo D, Mena-Rejon GJ, Cedillo-Rivera R, Quijano L (2008) 21beta-Hydroxy-oleanane-type triterpenes from *Hippocratea excelsa*. *Phytochemistry* 69: 1057-1064.
- Khalifah RG, Baynes JW, Hudson BG (1999) Amadorins: novel post-Amadori inhibitors of advanced glycation reactions. *Biochem Biophys Res Commun* 257: 251-258.
- Frye EB, Degenhardt TP, Thorpe SR, Baynes JW (1998) Role of the Maillard reaction in aging of tissue proteins. Advanced glycation end product-dependent increase in imidazolium cross-links in human lens proteins. *J Biol Chem* 273: 18714-18719.
- Furth AJ (1997) Glycated proteins in diabetes. *Br J Biomed Sci* 54: 192-200.